FATIGUE TESTS ON DEFECTIVE CIRCUMFERENTIAL WELDED PIPE JOINTS

T. Watanabe, Y. Hasegawa and K. Matsumoto

Safety and Inspection Engineering Center,

JGC CORPORATION, Yokohama, Japan

ABSTRACT

While research work concerning fatigue strength of welded joints containing defects is being extensively conducted in Japan, researchers are, in many cases using plane plate specimens or small size test pieces.
However, in consideration of the fact that piping joints are subject to complex changes in configuration and restrictive conditions, we believed it was problematical to evaluate defects based on abovementioned test results.
Therefore, we conducted bending fatigue tests using actual pipe welds containing incomplete penetration to investigate the fatigue crack growth and correlation between defect and fatigue life.
As a result, it was found that the crack growth behavior is similar to that under cyclic tensile load, and the number of loading cycles until a fatigue crack propagates throughout the wall thickness can be reasonably estimated using the stress intensity factor for the initial defect.

KEYWORDS

Fatigue test; Fatigue strength; Bending moment; Pipes; But joints, Carbon steels, Penetration defects, Crack propagation.

INTRODUCTION

Several welded structural failures are caused by fatigue. A large number of welded joints are used on piping and pressure vessels in chemical plants.
The effect of weld defects on the joint strength has been taken up for discussion in some reports (e.g. Ishii, 1967), in which it is shown that the fatigue strength is largely affected especially by cracks and incomplete penetration.
Since these experiments were conducted by using plane plate specimens, the relevance of evaluating welded joints in piping based on the data is debatable.
Therefore, our fatigue tests were conducted in conditions near to actual piping by using welded joints with incomplete penetration which is liable to occur in welding of piping, and the fatigue strength and crack growth behavior were investigated.

TEST SPECIMENS

3B (in nominal size) carbon steel pipes for high temperature service (JIS G 3456 STPT 38) were used and butt welded by gas tungsten arc welding (GTAW) for the first layer and shielded metal arc welding (SMAW) with low hydrogen type electrodes for the forward layers. Sound joints (test specimen symbol G) and defective joints (symbol B) with incomplete penetration throughout the internal circumference were welded for three different wall thickness pipes respectively. No stress relief was applied to the test specimens.
Details of the test specimens and welding conditions are shown in Table 1.
The chemical compositions and mechanical properties of the test specimens are shown in Table 2.

TABLE 1 Test Specimens and Welding Conditions

Test specimens		Materials	Welding conditions	Depth of incomplete penetration
40	G	STPT38 SCH40 89.1 mm o.d. 5.5 mmt	First layer: GTAW(TGS 50, 2.4ϕ) G type specimen 16.6 ~ 20.5 kJ/cm B type specimen 10.7 ~ 13.5 kJ/cm Forward layers: SMAW (LB 26, 3.2ϕ, 4.0ϕ) G type specimen 17.4 ~ 27.3 kJ/cm B type specimen 14.7 ~ 22.1 kJ/cm	No defect
	B			2.0 ~ 2.9 mm
80	G	STPT38 SCH80 89.1 mm o.d. 7.6 mmt		No defect
	B			1.5 ~ 3.1 mm
160	G	STPT 38 SCH160 89.1 mm o.d. 11.1 mmt		No defect
	B			1.2 ~ 3.2 mm

Configuration of the cross section of welds

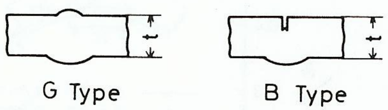

TABLE 2 Chemical Compositions and Mechanical Properties of Test Specimens

Materials	Chemical compositions (%)				
	C	Mn	Si	P	S
Base metal (STPT 38)	0.16	0.49	0.24	0.016	0.013
Weld metal (D 4316)	0.098	0.92	0.41	0.015	0.007

Materials	Mechanical properties		
	Yield strength σ_Y (N/mm^2)	Tensile strength σ_B (N/mm^2)	Elongation (%)
Base metal (STPT 38)	265	402	65
Weld metal (D 4316)	471	539	33

EXPERIMENTAL PROCEDURES

The fatigue test machine was devised for the experiment.
Figure 1 shows the fatigue test machine setting a test specimen. The weld side end of the test specimen was fixed and the other end was connected with the bar intended to convert the rotary motion of the motor into horizontal vibration, by which alternating bending load was given to the weld. The stress can be set for a desired value by changing the amplitude of vibration. The axial strain was measured by strain gauges at a distance of 15 mm from the weld. The cycle rate was 150 cycles per minute. All specimens were tested at room temperature.
From the fact that the defect was incomplete penetration, it was expected that the fatigue crack would propagate from the internal surface toward the external surface. Then, the failure termination time was detected as follows; pressurized rust inhibitor-water solution was put in the test specimen, and if the solution leaked out through the crack, the pressure dropped to stop the fatigue test machine automatically. The number of cycles are the rotations (150 cycles/min.) multiplied by the test time from start until stop.

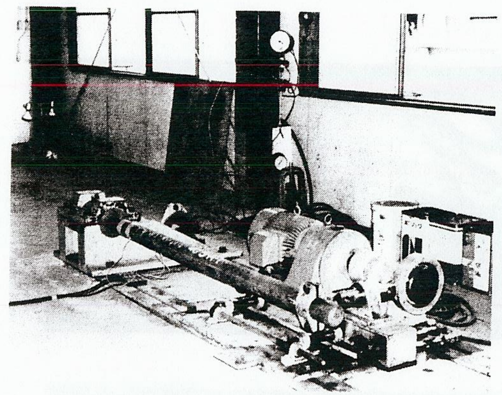

Fig. 1. The fatigue test machine and a test specimen.

EXPERIMENTAL RESULTS

Fatigue cracks initiated from the internal surface in all the test specimens including the sound specimens.
The fatigue test results are shown in the form of S-N diagram in Fig. 2, in which the ordinate stands for the stress (1/2 of the nominal stress range).
The values in the figure show the depth of incomplete penetration of each specimen.
The fatigue life is remarkably different between defective welds and sound welds. Around 2 x 10^6 cycles, the fatigue strength of the defective welds is about 1/2 of that of the sound welds. The fatigue limit of sound welds appeared about to be 60 N/mm^2, on the other hand, the defective test specimen with 1.2 mm incomplete penetration did not initiate any fatigue crack until 4.3 x 10^6 cycles at 34 N/mm^2.
Figure 3 shows an instance of fatigue crack shapes in the sound and defective welds. The fatigue crack initiated from the root of the weld in the sound welds, on the other hand, it started at the bottom of the incomplete penetration in the defective welds.
In both cases, the fatigue crack propagated radially from inside toward outside of pipes, but with respect to the shape, defective welds had greater propagation in

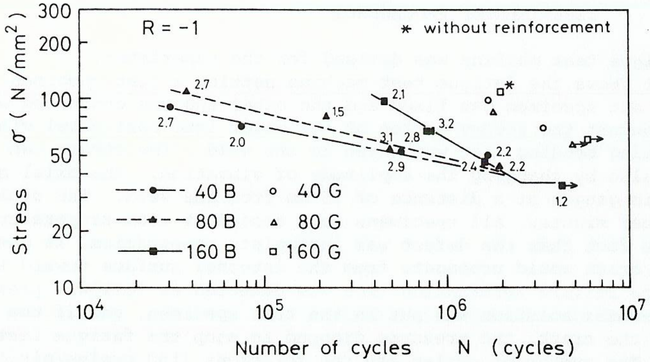

Fig. 2. S-N diagrams of experimental results

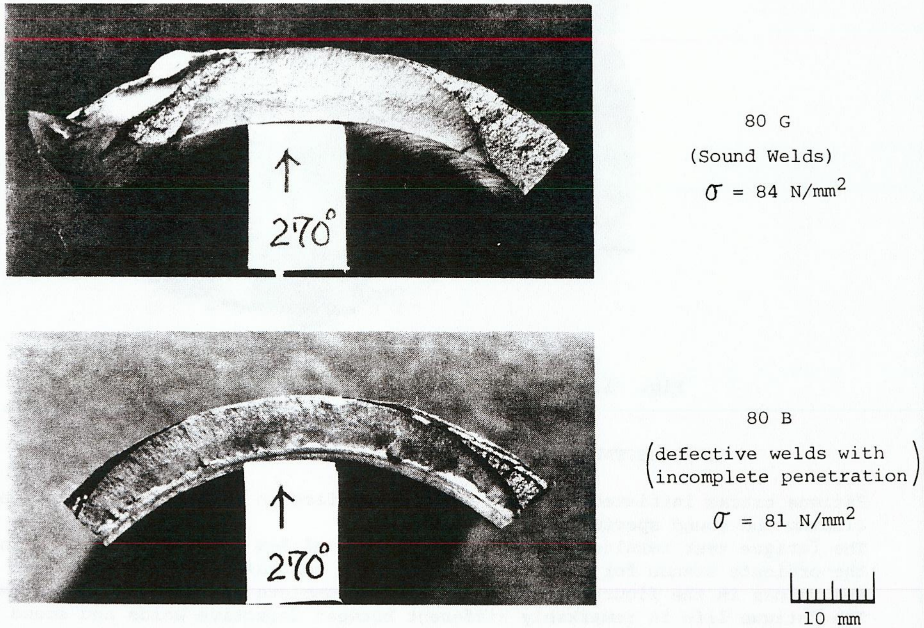

Fig. 3. Difference of fatigue crack shapes between sound welds and welds with incomplete penetration.

the circumferential direction compared with sound welds.
The behavior of the fatigue crack growth was examined on 160B test specimens. Figure 4 shows the relation between the fatigue crack length and the number of cycles.

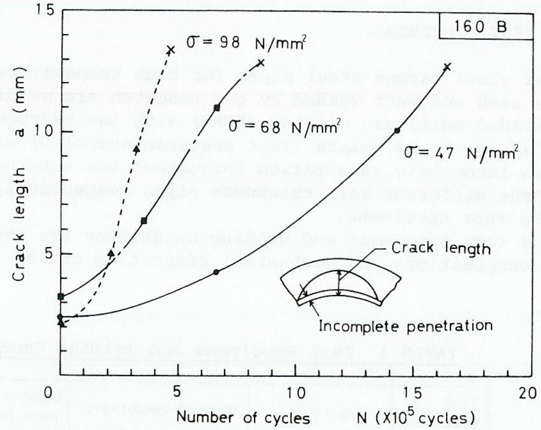

Fig. 4. Crack propagation curves.

The crack length including the depth of the incomplete penetration was measured by the beach marks provided on the fracture surface during the fatigue test.
As shown in the figure, the higher the stress was, the faster the growth rate was, and it is suggested that the fatigue crack initiated at an early stage of the fatigue life.

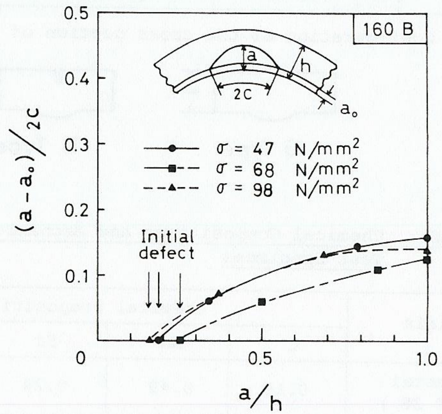

Fig. 5. Changes in crack shapes.

Figure 5 shows the relation between the depth of fatigue crack and the aspect ratio of the cracks. In this case, 2c of the ordinate in this figure was measured along the bottom of the incomplete penetration. The aspect ratio increases gradually with the growth of the crack, however the degree of the increase decreases as the crack is extending toward the external surface.
This fact is different from a phenomenon which has been observed generally in a plane plate test specimen under bending load. Hence, it became evident that, even

if a pipe was subjected to bending load, the fatigue crack of a pipe welded joint showed the same crack growth behavior as subjected to tension.
This fact is easily understood from the stress distribution at the cross section of these pipes subjected to bending load.

DISCUSSION

Regarding fatigue tests, numerous data have been presented to date, but in many cases the complicated configurations of welded structures prevented analysis of fatigue crack growth behavior and estimation of life by these data. In this experiment, the testing was intended to be conducted in conditions as near as possible to actual piping.
As stated before, all fatigue cracks started at the inside of the test specimens. It is easily understood that cracks start at the bottom of the incomplete penetration in the case of the defective welds. However, in the case of the sound welds it is hard to understand why cracks start at the internal surface, if considering the stress distribution at the cross section of a pipe by bending load.
The geometrical discontinuity is one of factors for crack initiation. In this case, comparing the geometry of the face reinforcement and the root, it is supposed that higher stress concentration occurred at the root of welds. Also, it is considered that the crack initiation was affected by residual stresses, because they are compressive on the pipe external surface and tensile on the pipe internal surface.
Meanwhile, regarding the difference of the fatigue crack shape between defective welds and sound welds, it is seemed to depend on the configuration of the root of welds. That is, defective welds have chances for fatigue cracks to initiate from several points, compared with sound welds.
Therefore in case of actual piping, it is likely that a big area of fatigue crack in defective welds make it easier to translate to other types of failures than sound welds.
On the other hand, the reason why the behavior of crack growth was closely similar to that subjected to cyclic tensile load, is as follows. If the stress at the cross section of a pipe is regarded as a composite of tensile and bending stresses, the component of the bending stress is small, compared with that of the tensile stress, because the pipe wall thickness is thin compared with the pipe diameter.
We tried to get the relation between the stress intensity factor range and the fatigue crack growth rate from the results of our tests.
The stress intensity factor was calculated by using the following formula (on the tensile load) which is one of the formula proposed by R.C. Shah and A.S. Kobayashi (1972).

$$\Delta K = 2/\pi \cdot M_t \cdot \Delta\sigma_T \cdot \sqrt{\pi a} \qquad (1)$$

Where, M_t = stress intensity magnification factors at the point of maximum crack depth for surface cracks in tension
$\Delta\sigma_T$ = tensile stress component
a = crack length from the internal surface

$\Delta\sigma_T$ is calculated as the average value of the stresses at the pipe internal and external surfaces.
The crack growth rate is calculated from Fig. 4 as the average value for the length of the crack growth at the beach mark points during 5 x 10^4 cycles. The results are shown in Fig. 6.
The relation between da/dN and ΔK will be represented by the solid line, and in this case the values m and C of the following Paris' power law are 1.67 and 1.77 x 10^{-9} respectively.

$$da/dN = C\,(\Delta K)^m \qquad (2)$$

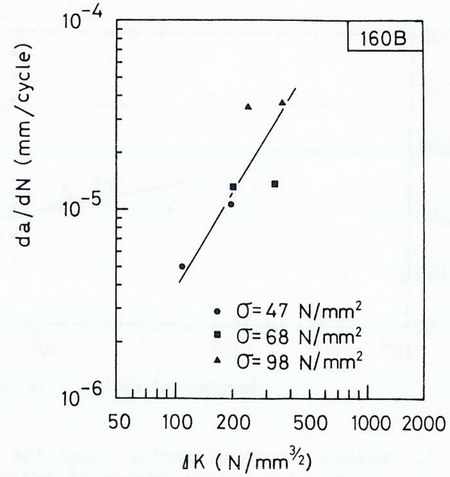

Fig. 6. Crack growth rate versus stress intensity factor range.

These values correspond with the relation between m and C which Kitagawa (1972) has reported.
Also, we tried to obtain the relation between the depth of incomplete penetration and fatigue life by using the stress intensity factor range, which is Tada's formula (1973) for the single edge notched strip, regarding the incomplete penetration as the initial crack. Since the formula is resolved for a crack in a plane plate, the value is shown especially as ΔK_{IP} herein.

$$\left.\begin{aligned} \Delta K_{IP} &= \Delta\sigma_T \cdot \sqrt{\pi a_o} \cdot F(a_o/t) \\ F(a_o/t) &= \sqrt{2t/\pi a_o \cdot \tan(\pi a_o/2t)} \cdot \left[0.752+2.02(a_o/t)+0.37\{1-\sin(\pi a_o/2t)\}^3\right] \\ &\quad \times 1/\cos(\pi a_o/2t) \end{aligned}\right\} \qquad (3)$$

where, $\Delta\sigma_T$ = tensile stress component
a_o = depth of incomplete penetration
t = plate thickness including the face reinforcement

The results are shown in Fig. 7. From this figure, there seemed to be some relation between the fatigue life and the depth of incomplete penetration, and it will be possible to estimate the fatigue life by ΔK_{IP}, though roughly.

CONCLUSION

Alternating bending fatigue tests were conducted on carbon steel pipes with a circumferential butt welded joint. The following results were obtained with respect to fatigue cracks which initiated from the incomplete penetration.

1) Fatigue cracks started at inside of the pipe and propagated radially regardless

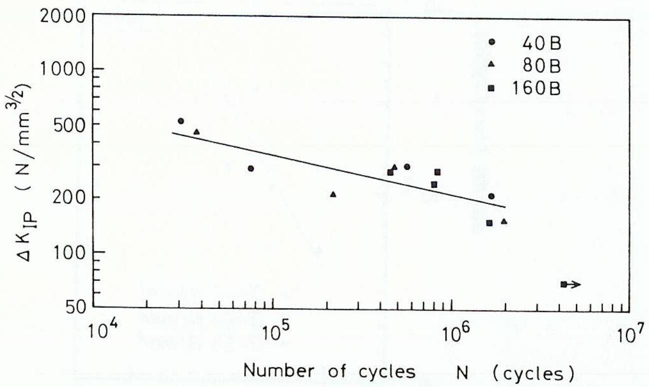

Fig. 7. Stress intensity factor range for incomplete penetration versus number of cycles at fatigue crack penetrating through welds.

of whether there were defects at inside or not.

2) The behavior of the fatigue crack growth in a pipe subjected to cyclic bending load is similar to axial tensile stress.
3) Fatigue cracks of welds containing incomplete penetration propagated wider toward the circumferential direction compared with sound welds.
4) With respect to the relation between the fatigue crack growth rate and stress intensity factor range, the factors C and m in Paris' power law corresponded with the relation which have been reported.
5) There seemed to be some relation between the depth of incomplete penetration and fatigue life, and the fatigue life will be estimated by stress intensity factor range for incomplete penetration.

REFERENCES

Ishii, Y., H. Kihara, and Y. Tada (1967). On the Relation between the Non-destructive testing Information of Steel Welds and their Mechanical Strength. Journal of N. D. I. (Japan), 16, 319-345.

Kitagawa, H. (1972). Application of Fracture Mechanics to Fatigue Crack. (Japanese) Journal of the J. S. M. E. (Japan), 75, 642, 1068-1080.

Shah, R. C. and A. S. Kobayashi (1972). Stress Intensity Factor for an Elliptical Crack Approaching the Surface of a plate in Bending. ASTM STP 513, (1).

Tada, H., P. C. Paris and G. R. Irwin (1973). The Stress Analysis of Cracks HandBook., 2.10.